Fast-Deactivating Calcium Channels in Chick Sensory Neurons

D. SWANDULLA and C. M. ARMSTRONG

From the Department of Neurophysiology, Max Planck Institute for Psychiatry, D-8033 Martinsried-Planegg, Federal Republic of Germany, and Department of Physiology, University of Pennsylvania, School of Medicine, Philadelphia, Pennsylvania 19104

ABSTRACT Whole-cell Ca and Ba currents were studied in chick dorsal root ganglion (DRG) cells kept 6–10 h in culture. Voltage steps with a 15-μs rise time were imposed on the membrane using an improved patch-clamp circuit. Changes in membrane current could be measured 30 μs after the initiation of the test pulse. Currents through Ca channels were recorded under conditions that eliminate Na and K currents. Tail currents, associated with Ca channel closing, decayed in two distinct phases that were very well fitted by the sum of two exponentials. The time constants τ_f and τ_s were near 160 μs and 1.5 ms at -80 mV, 20°C. The tail current components, called FD and SD (fast-deactivating and slowly deactivating), are Ca channel currents. They were greatly reduced when Mg^{2+} replaced all other divalent cations in the bath. The SD component inactivated almost completely as the test pulse duration was increased to 100 ms. It was suppressed when the cell was held at membrane potentials positive to -50 mV and was blocked by 100–200 μM Ni^{2+}. This behavior indicates that the SD component was due to the closing of the low-voltage–activated (LVA) Ca channels previously described in this preparation. The FD component was fully activated with 10-ms test pulses to $+20$ mV at 20°C, and inactivated to ~30% during 500-ms test pulses. It was reduced in amplitude by holding at -40 mV, but was only slightly reduced by micromolar concentrations of Ni^{2+}. Replacement of Ca^{2+} with Ba^{2+} increased the FD tail current amplitudes by a factor of ~1.5. The deactivation kinetics did not change (*a*) as channels inactivated during progressively longer pulses or (*b*) when the degree of activation was varied. Further, τ_f was affected neither by changing the holding potential nor by varying the test pulse amplitude. Lowering the temperature from 20 to 10°C decreased τ_f by a factor of 2.5. In all cases, the FD component was very well fitted by a single exponential. There was no indication of an additional tail component of significant size. Our findings indicate that the FD component is due to closing of a single class of Ca channels that coexist with the LVA Ca channel type in chick DRG neurons.

INTRODUCTION

Two types of Ca channels have now been suggested or demonstrated in a variety of tissues, including egg cells (Hagiwara et al., 1975; Fox and Krasne, 1981, 1984),

Address reprint requests to Dr. D. Swandulla, Max Planck Institute for Psychiatry, Dept. of Neurophysiology, Am Klopferspitz 18A, D-8033 Martinsried-Planegg, Federal Republic of Germany.

J. GEN. PHYSIOL. © The Rockefeller University Press · 0022-1295/88/08/0197/22 $2.00
Volume 92 August 1988 197–218

neuroblastoma cells (Fishman and Spector, 1981; Narahashi et al., 1987), endocrine cells (Matteson and Armstrong, 1984*a*, 1986; Armstrong and Matteson, 1985; Cota, 1986; DeRiemer and Sakmann, 1986), ciliates (Deitmer, 1984), vertebrate heart muscle (Bean, 1985; Nilius et al., 1985; Mitra and Morad, 1986), and vertebrate neurons (Llinas and Sugimori, 1980; Llinas and Yarom, 1981; Carbone and Lux, 1984*a*, *b*; Nowycky et al., 1985*a*; Fedulova et al., 1985; Bossu et al., 1985). The two types of Ca channels exhibit different thresholds for activation. One type, called the low-voltage–activated (LVA) or T channel in chick dorsal root ganglion (DRG) neurons, turns on between −50 and −30 mV, while the other one, called the high-voltage–activated (HVA) or L channel, activates between −20 and 0 mV. In the presence of intracellular Ca^{2+} chelators, LVA channels inactivate faster than HVA channels, which resemble the classic Ca channels described in numerous other preparations (for review, see Hagiwara and Byerly, 1981).

Recently, the existence of a third type of Ca channel, the N channel, was postulated in chick DRG cells on the basis of macroscopic and single-channel current recordings (Nowycky et al., 1985*a*). The N channel currents were distinguished from the other Ca currents on the basis of the voltage range over which they activate, their rate of inactivation, and their pharmacological properties and single-channel conductance (8, 13, and 25 pS for T, N, and L channels with 110 Ba^{2+} outside; Nowycky et al., 1985*a*). Carbone and Lux (1987*b*) also saw more than two conductance levels with isotonic Ba^{2+}, but suggested that two of these arise from a single channel type, HVA, one of the levels being a subconducting state.

We felt that clarification of these matters might come from the study of tail currents. Tail current analysis has proved to be helpful in distinguishing two types of Ca channels in clonal pituitary cells (Matteson and Armstrong, 1984*a*, 1986; Armstrong and Matteson, 1985) and pituitary pars intermedia cells (Cota, 1986). Ion channels activated by depolarization close or "deactivate" upon repolarization as their voltage-dependent activation gates close. A typical channel continues to carry current for a fraction of a millisecond after repolarization, giving rise to a "tail" current, the time course of which reflects the kinetics of the closing process. In GH_3 and pituitary cells, the two Ca channel populations deactivate with distinct kinetics and are easily separated.

We employed tail current analysis in chick DRG neurons in various conditions with the idea that a possible third Ca channel type might have distinct deactivation kinetics. If, for instance, N channels inactivate completely during sustained depolarization and HVA (L) channels do not (see Nowycky et al., 1985*a*), then the tail current kinetics should change after N channel inactivation. Using this method, we identified fast-deactivating and slowly deactivating Ca channels with properties similar to HVA and LVA channels. We found no evidence in macroscopic current recordings for the existence of a third type of Ca channel in this preparation.

Part of this work has already appeared in a short report (Swandulla and Armstrong, 1987).

METHODS

Culture

The experiments were performed on primary cultures of chick DRG cells. Sensory ganglia were dissected from the lumbar region of 8–13-d-old chick embryos (*Gallus domesticus*). Gan-

glia were dissociated into single cells by a 15–30-min incubation at 37°C in Ca^{2+}-free Spinner's salt solution (Sigma Chemical Co., St. Louis, MO; HEPES-buffered to pH 8.0) containing 0.1% trypsin and gently triturated. Dissociated cells were plated on slivers of coverslips coated with collagen or poly-D- or -L-lysine and maintained in a CO_2 incubator at 37°C in minimal Eagle's medium (Gibco Laboratories, Grand Island, NY) supplemented with 10% horse serum (Gibco Laboratories), 2% of 0.3 g/ml glucose, and 2% of 30 mg/ml L-glutamine. In some experiments, 100 U/ml penicillin and 100 μg/ml streptomycin (Flow Laboratories, Inc., McLean, VA) were added to the culture medium. Nerve growth factor (Sigma Chemical Co.; 5 μg/ml) was occasionally added. Neither antibiotics nor nerve growth factor had a measurable effect on the tail current kinetics.

Solutions

The composition of the solutions used is given in Table I. In the text, solutions are specified as external//internal. Unless otherwise specified, the anion was Cl. All solutions were filtered

TABLE I

Solutions

External cations	Choline chloride	$CaCl_2$	$BaCl_2$	$MgCl_2$		
mM	*mM*	*mM*	*mM*	*mM*		
5 Ca^{2+}	140	5		2		
	140	10		10		
20 Ca^{2+}	120	20		2		
	135	20		2		
5 Ba^{2+}	140		5	2		
	140		5	10		
	150		5			
10 Ba^{2+}	140		10	2		
15 Mg^{2+}	140			15		
Internal cations	CsCl	NMG-Cl	TEA-Cl	$MgCl_2$	EGTA	BAPTA
50 Cs^+	50	50	20	2	10	
	50	50	20	2		10
	50	30	20	2		20

The osmolarity of all solutions was adjusted to ~300 mosmol. NMG was titrated with HCl to pH 7.0. EGTA and BAPTA were used as Cs salts. All solutions were buffered with 10 mM HEPES. The pH was adjusted to 7.3 by adding Cs(OH).

through 0.22-μm cellulose acetate filters (Corning Glass Works, Corning, NY). External solutions were normally Na^+- and K^+-free, and 1–3 μM tetrodotoxin (TTX; Sigma Chemical Co.) was added in several experiments to suppress Na currents.

Recording Conditions

Neurons were used for whole-cell current recordings 6–12 h after plating. At this culture stage, cells are round and most of them are free of processes. Coverslips were transferred from 35-mm culture dishes to the recording chamber, which contained 0.3 ml of external recording solution and was continually exchanged by a flow/suction device. Solution exchange was complete in ~30 s. Seal resistances of ~1–5 GΩ were easily formed with most of

the solutions used. Pipettes were fabricated from Kimax-51 borosilicate capillary tubes and had resistances between 0.45 and 1.5 MΩ.

Electronics

The patch-clamp amplifier for whole-cell current recording includes most of the features described by Hamill et al. (1981). We used an OPA 111 (Burr-Brown Research Corp., Tucson, AZ) with a 10-MΩ feedback resistor as the current-to-voltage converter. This low feedback resistance improves the time resolution for monitoring current at the expense of increasing noise, which was not critical for our experiments. The speed with which a voltage step could be applied to the cell membrane was enhanced by a technique described in detail by Armstrong and Chow (1987) that uses the normal head-stage configuration described by Hamill et al. (1981), but alters the command voltage applied to the positive input of the amplifier. Large voltage spikes of 15 μs duration were added to the leading edge of the command steps to charge the membrane capacitance rapidly. The spike amplitude was determined by nulling the slow capacitive transient (typical time constant, 50 μs) that appeared on

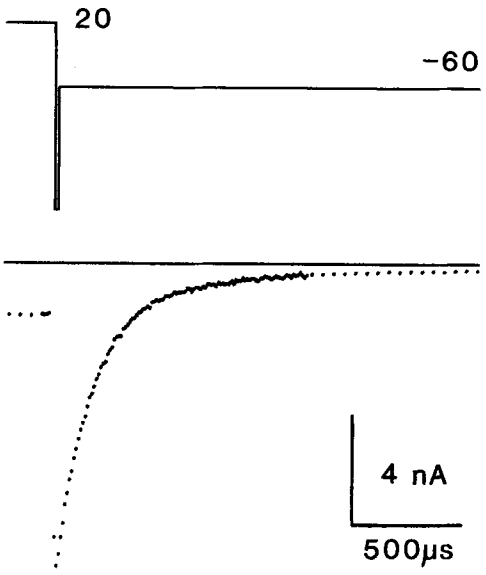

FIGURE 1. Time resolution of tail current measurements. Ca currents were activated by 10-ms steps from −80 to +20 mV. Repolarization was to −60 mV. The upper trace shows the voltage change during the repolarization phase of a test pulse. The repolarizing step has a 24-mV voltage spike of 15 μs duration on its leading edge. The lower trace shows the corresponding tail current recording. The sample rate was 10 μs per point. The electrode resistance was 0.6 MΩ. Series resistance compensation was 0.4 MΩ. 10 Ca^{2+}, 10 Mg^{2+}, 1 μM TTX//50 Cs^{+}, 50 NMG^{+}, 10 EGTA. 20°C.

breaking into the cell. Because the access resistance normally changed during the experiment, spike amplitudes were readjusted every few minutes or when a new series of test pulses was started. Fig. 1 illustrates the time resolution of this procedure. Ca tail current was measured on repolarization to −60 mV after a 10-ms activating pulse from −80 to +20 mV. A voltage spike of 240 mV amplitude and 15 μs duration charged the membrane capacitance rapidly when the voltage was changed. Current measurements started 30 μs after initiation of the voltage step. The sample rate was 10 μs per point for tail measurements.

Data Aquisition

An LSI-11/73 computer (Digital Equipment Corp., Marlboro, MA) was used to acquire, store, and analyze the data. The interface between the analog electronics and the computer was made as described in Matteson and Armstrong (1984*b*). The sample rate was 10, 20, or 200 μs per sample point. Currents were corrected by subtracting linear components of capac-

itive and ionic current. For this purpose, 10 current responses to 50-mV hyperpolarizing pulses from the holding potential were averaged to give a control trace, which was scaled and subtracted from the test current. The control trace was refreshed at frequent intervals.

Exponential Curve-Fitting

The time course of the tail currents could be well fitted by the sum of two exponentials, using a least-squares procedure. The slow component was determined by fitting the latter part of the trace after the fast component had decayed away. The fitted slow exponential was extrapolated to the beginning of the step and subtracted from the original current trace. The remaining fast tail current was then fitted with a second least-squares exponential. The amplitude of the fast component was measured either as the initial amplitude of the current remaining after subtraction of the slow exponential or as the measured amplitude of the current remaining after subtraction of the slow exponential.

RESULTS

Ca Channel Currents in Chick DRG Neurons

The solutions used in our experiments were designed to isolate membrane currents through Ca channels. Fig. 2 shows the voltage-dependent inward currents carried by Ca or Ba ions recorded under these experimental conditions. During 10-ms step depolarizations from the holding potential (−80 mV), the currents activated with a sigmoidal time course and reached their maximum amplitude within several milliseconds. The time to peak was dependent on the size of the test pulse and decreased about e-fold for a 54-mV change in membrane potential at 20°C, as determined with longer test pulses. Time-dependent outward currents were very small even with large depolarizing steps (not illustrated), which indicated that K currents were successfully suppressed. A fairly large initial transient of outward current, as in the records of Fig. 2, was not investigated in detail. Similar currents have been recently described and interpreted as Ca channel gating currents (Kostyuk et al., 1977; Adams and Gage, 1977).

The currents that activated during membrane depolarization deactivated on repolarization. The current jumped in magnitude because of the increased driving force when stepping back to −80 mV after the test pulse. At this negative potential, the voltage-dependent activation gates of the channels closed, giving rise to a "tail" current that decayed in magnitude as the channels deactivated. This is illustrated in Fig. 2 for repolarizations following activating pulses to +10 mV with Ca and Ba ions as charge carriers.

Tail Currents Show Evidence for Two Types of Ca Channel

The tail currents clearly decayed in two phases and could be fitted very well by a sum of two exponentials (Fig. 3). In Ca^{2+} solutions, the fast time constant was near 160 μs at 20°C, about one order of magnitude smaller than the slow one at this temperature. In Ba^{2+} solutions, the fast tail component was found to be slightly slower than in Ca^{2+} (see Fig. 3), a point to be investigated in more detail in another study. When the holding potential was changed from −80 to −50 mV or more positive, the slow tail component vanished. It was also strongly reduced when 100–200 μM Ni^{2+} was added to the external solution. Ni^{2+} has been shown to selectively

block the LVA currents in this preparation (Carbone et al., 1987). In both cases, the decay kinetics of the fast tail component were unchanged. These findings indicate that the slow tail component was due to deactivation of LVA channels, which we will call here slowly deactivating (SD) in contrast to the fast-deactivating (FD) Ca channels, represented by the fast tail current component.

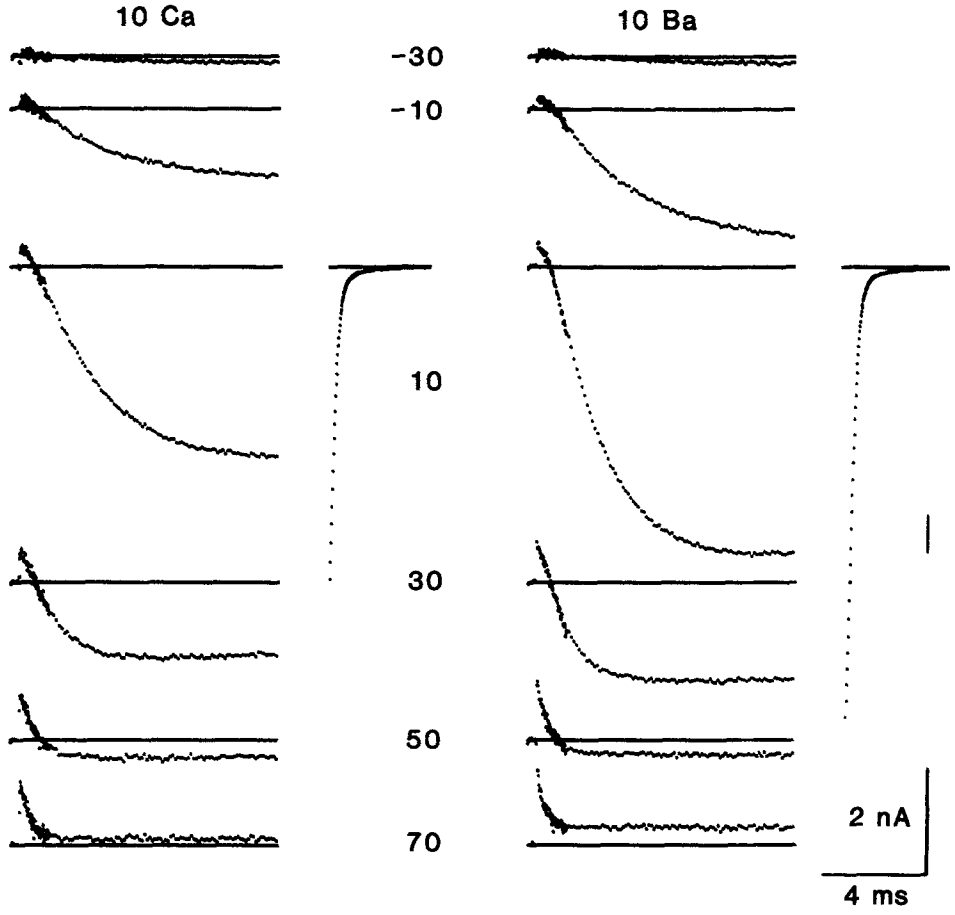

FIGURE 2. Whole-cell Ca and Ba currents through Ca channels recorded at the membrane potentials indicated (single cell). 10-ms test pulses were from −80 mV. Ba current recordings were started 60 s after changing the external solution from 10 mM Ca^{2+} to 10 mM Ba^{2+}. The cell diameter was 23 μm. Note different current scales for tail currents (upper bar). 10 Ca^{2+}/10 Ba^{2+}, 2 Mg^{2+}//50 Cs^{+}, 50 NMG^{+}, 10 BAPTA. 20°C.

Replacing Ba^{2+} with Mg^{2+} in the external medium (Fig. 4) or adding Ni^{2+} in higher concentrations (5 mM) to the external solution almost completely blocked the pulse current and substantially reduced both tail current components reversibly. The remaining tail currents, as shown for Mg^{2+} in Fig. 4, may be due to Mg^{2+} through Ca channels, but this possibility was not further investigated.

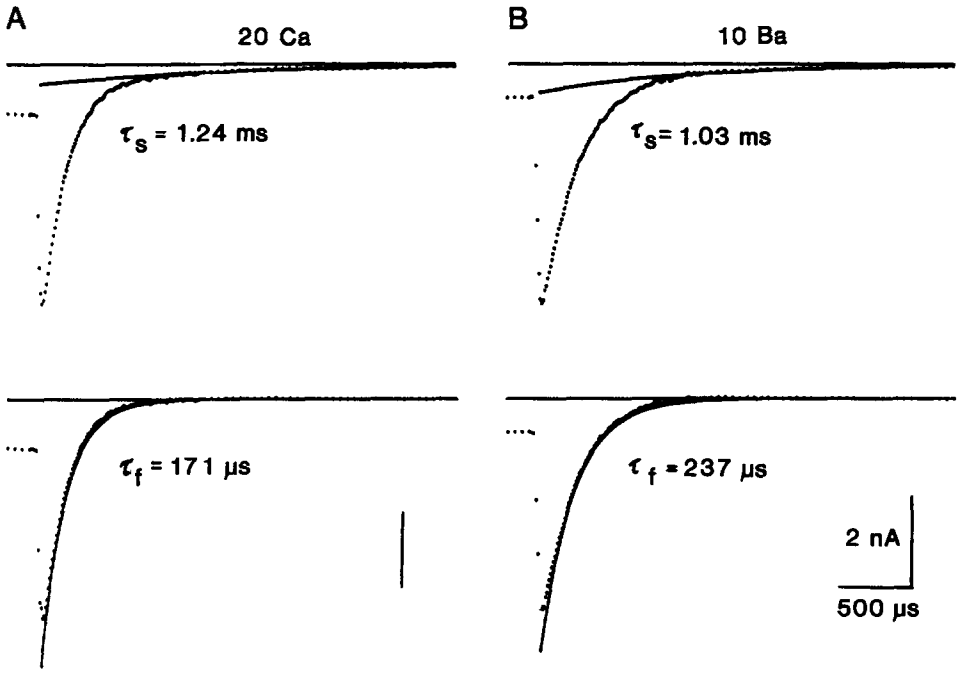

FIGURE 3. Ca channel tail currents carried by Ca and Ba ions. Tail currents were recorded on repolarization to −60 mV after 15-ms test pulses from −80 to +20 mV. The continuous curves in *A* and *B* (upper traces) are single exponentials fitted to the slow component of each tail. After subtracting out the slow component (lower traces), the fast component was fitted with a single exponential (continuous curves in lower traces). Time constants were as indicated. (*A*) 20 Ca^{2+}, 2 Mg^{2+}//50 Cs^+, 30 NMG^+, 20 BAPTA, 18°C, (*B*) 10 Ba^{2+}, 2 Mg^{2+}//50 Cs^+, 30 NMG^+, 20 BAPTA. 20°C.

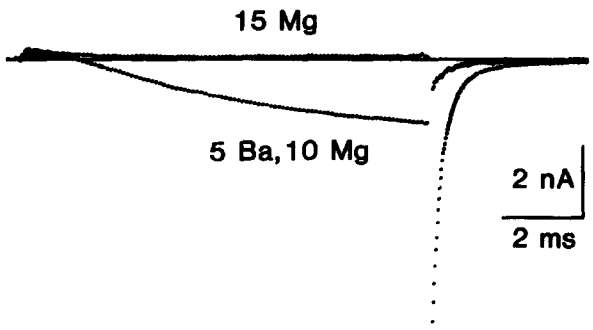

FIGURE 4. Reduction of Ca current by Mg^{2+}. When the external solution was changed from 5 Ba^{2+}, 10 Mg^{2+} to 15 Mg^{2+}, the pulse current was almost completely blocked and the tail current components were substantially reduced. Changing back to 5 Ba^{2+}, 10 Mg^{2+} almost completely restored pulse and tail currents. Traces before and after 15 Mg^{2+} were averaged. Test pulses were from −80 to +20 mV with a return to −60 mV. 5 Ba^{2+}, 10 Mg^{2+}//50Cs^+, 50 NMG^+, 10 BAPTA. 20°C.

In most of the cells, the fast tail component had an amplitude that was about one order of magnitude larger than the slow one. The ratio of the two amplitudes was even larger when Ba^{2+} was substituted for Ca^{2+} in the external bathing solution. This observation suggests that FD channels conduct Ba ions better than Ca ions, a point further investigated below. These tail current properties made it easy to study the FD tail component in sufficient isolation, even when SD current tails were not suppressed by one of the measures described above. The following results will concentrate on FD currents.

Current-Voltage Relations of FD Channels

Currents through Ca channels were recorded in 5 mM extracellular Ca^{2+} or Ba^{2+}, and Fig. 5 shows current amplitude as a function of voltage. In this cell, there were

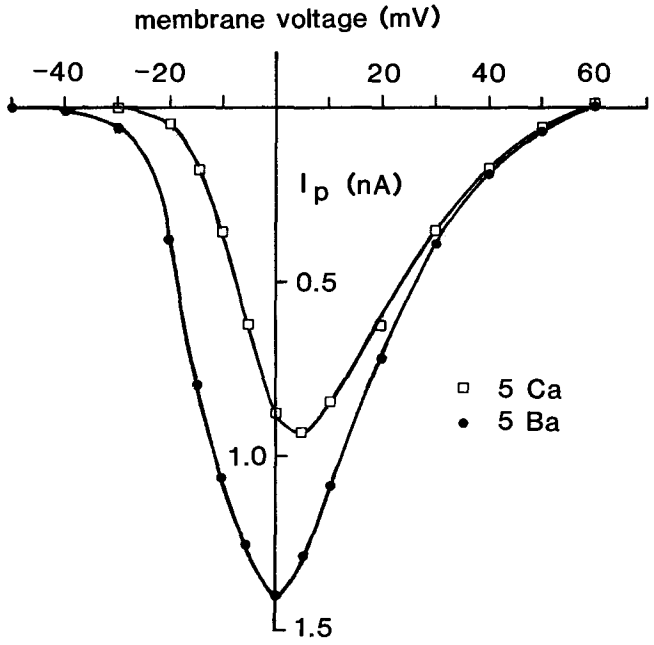

FIGURE 5. Normalized peak Ca and Ba currents plotted against membrane potential (same cell). Note that there is no indication for the presence of LVA channels in this cell. Peak currents recorded in 5 mM Ba^{2+} before and after changing the external solution to 5 mM Ca^{2+} were averaged. Test pulses of 13 ms duration were from −80 mV holding potential. 5 Ca^{2+}//5 Ba^{2+}, 2 Mg^{2+}//50 Cs^{+}, 50 NMG^{+}, 10 BAPTA. 15°C.

very few LVA channels and no peak in the current-voltage (*I-V*) curve near −20 mV. The records were taken in 5 mM Ba^{2+}, after changing to 5 mM Ca^{2+}, and on return to 5 mM Ba^{2+}. The before and after traces in Ba^{2+} were very similar, and the plotted peak currents are their average. In experiments where the series resistance error was eliminated by electronic compensation, the *I-V* curve in Ba^{2+} was shifted to the left along the voltage axis by 5–10 mV relative to the Ca^{2+} curve. The peak

current amplitude rose sharply between −15 and +5 mV in Ca^{2+} and between −20 and 0 mV in Ba^{2+}, and then declined again to approach the voltage axis. Above +60 or 70 mV, the current was outward. Its magnitude was not more than 1/10 that of the maximum inward current, even up to +100 mV, when Cs^+ was the major internal cation, and it was substantially smaller with Cs^+/NMG^+ mixtures. With NMG^+ as the major internal cation (no Cs^+), pulse currents remained inward even up to +100 mV. Thus, it appeared likely that Cs^+ was the carrier of the outward current by way of either Ca or K channels at potentials higher than +60 mV (see also Fenwick et al., 1982).

Ca^{2+}/Ba^{2+} Conductivity of FD Channels

The Ca^{2+} and Ba^{2+} conductivity of FD channels was also investigated in the experiment of Fig. 5. The maximum pulse current amplitude was larger in Ba^{2+} by a factor of ~1.5, as were the amplitudes of the tail currents (see Fig. 2). In neither Ca^{2+} nor Ba^{2+} was there evidence for more than a single component in the fast tail current. A slow tail component was absent in this neuron, as expected from the lack of LVA channel currents (see above).

Inactivation of FD Channel Currents

Inactivation was evident as decay of the current from its peak during a sustained depolarization (Fig. 6 *A*). Inactivation was never complete, even with 500-ms test pulses. The early decay of the pulse currents could be fitted with a single exponential, as illustrated in Fig. 6 *A*. With steps to +20 mV, the time constant of the current decay was near 100 ms at 20°C and increased slightly with more positive potentials. While the time constant was fairly regular in all cells investigated, the degree of inactivation was more variable. On the average, final currents were 30% of the peak value with 500-ms test pulses. This variability, which was not investigated in detail here, could not be attributed to current-dependent inactivation, since there was no correlation between the peak current amplitude and the degree of inactivation.

Inactivation was confirmed by FD tail current measurements, as shown in Fig. 6 *B*. Repolarizing the membrane after test pulses of increasing duration gave rise to tail currents of decreasing amplitudes. The tails are a direct measure of the fraction of channels not inactivated in the course of the depolarizing pulse. Their decreases in amplitude were always proportional to the decrease in pulse current owing to inactivation, as can be seen by comparing panels *A* and *B* of Fig. 6.

Fig. 6 *C* illustrates the time course of inactivation measured by the decay of tail current amplitudes after test pulses of increasing duration to +20 mV. In this case, the decline in current amplitude could be fitted with a single exponential, although slower components of inactivation are sometimes evident. The time constant of 90 ms compared well with that of the pulse current decay (97 ms) during the sustained test pulse to the same potential (Fig. 6 *A*).

How Many Components in the Fast Tail?

We employed two tests to see whether contributions from more than one channel type could be discovered in the fast tail current (after removing the contribution of the LVA current).

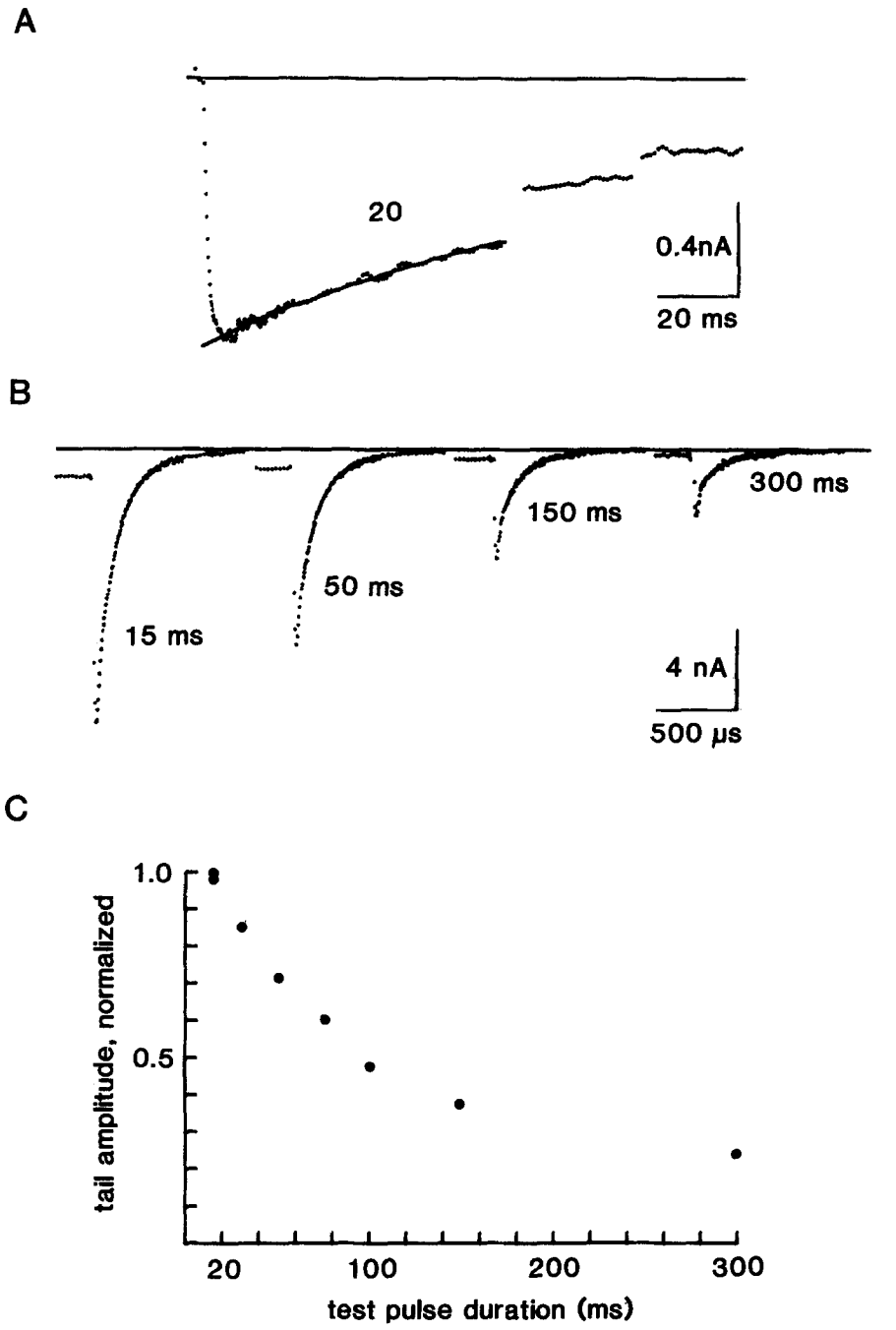

FIGURE 6. Tail currents and Ca channel current inactivation. *A* illustrates the decay of Ca channel current during a sustained (300 ms) test pulse from −80 to +20 mV. Sampling was interrupted between 80 and 160 ms, and between 190 and 270 ms for 80 ms. A single exponential with a time constant of 97 ms is fitted to the early current decay (solid line), which was assumed to reach steady state at the end of the test pulse. (*B*) Tail currents recorded on repolarization to −60 mV after pulses from −80 to +20 mV, for the durations indicated. Tails recorded after 15-ms pulses at the beginning and at the end of the series are superimposed, demonstrating almost full recovery of the current. Tail current amplitudes were normalized to the tail amplitude at 15 ms and plotted against test pulse duration (*C*). A single exponential (not shown) with a time constant of 90 ms could be fitted to the decay of the tail current amplitudes. 5 Ba^{2+}, 10 Mg^{2+}//50 Cs^{+}, 50 NMG^{+}, 10 BAPTA. 20°C.

(*a*) The first test was a search for more than one exponential component in the tail. Fig. 7 (left) shows the fit of a single exponential to the 15-ms tail from Fig. 6 *B*. The fit is very good, and the residual current (the low-amplitude trace, which is the difference between the experimental and the fitted curve) is extremely small, which suggests that there is no second exponential component of significant size. To further examine this point, two exponentials plus baseline were fitted to the trace, using a Fletcher-Powell routine. With 95% confidence, the routine assigned an amplitude of zero to the second component. Thus, with 95% confidence, the fast tail is a single exponential.

(*b*) In any case, the existence of more than one component could be the result of either two channel types or a single one with complex kinetics. Consequently, the

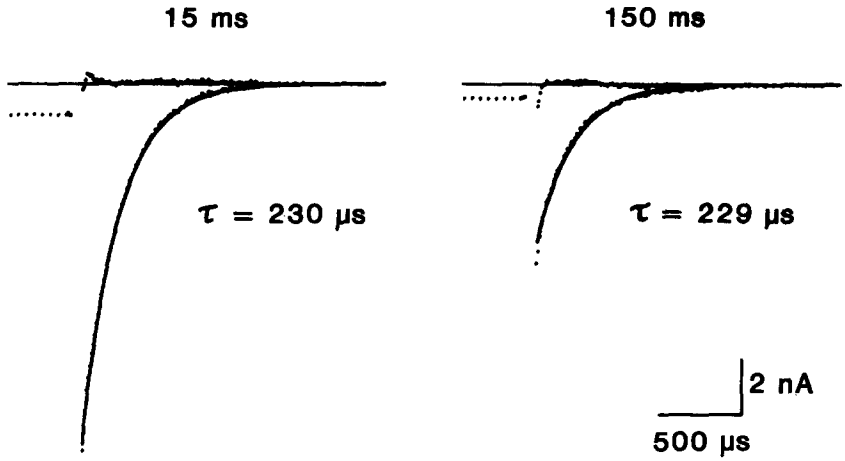

FIGURE 7. Tail current kinetics in the course of current inactivation. Same experiment as in Fig. 6 *B*. Tail currents were recorded on repolarization to −60 mV after activating pulses to +20 mV for the durations indicated. The continuous curves are single exponentials fitted to the fast component of each tail. Time constants were as indicated. The upper traces show the residual currents left after subtracting the fitted curves from the tail currents. A slow component was fitted with a single exponential (τ_s = 1.089 ms) and subtracted out before fitting the fast tail components. The amplitudes of fast and slow components were 13.57 and 0.43 nA (15-ms tail), and 6.6 and 0.11 nA (150-ms tail). 5 Ba^{2+}, 10 Mg^{2+}//50 Cs^{+}, 50 NMG^{+}, 10 BAPTA. 20°C.

more important test was to see whether the kinetics changed as the channels inactivated. According to the N channel hypothesis, N channels should be fully inactivated after 150 ms of depolarization (Nowycky et al., 1985*a*). Unless the deactivation rates of the N channels and the HVA channels are identical, the tail kinetics would be expected to change as the N channel contribution diminishes. In fact, the tail kinetics did not change as the current inactivated, as can be seen by comparing the two parts of Fig. 7. The best-fitting single exponential to the 150-ms tail, when many channels are inactivated, has the same time constant as the 15-ms tail (230 and 229 μs, respectively). As for the 15-ms tail, the residual current for the fit to the 150-ms tail is very small.

Additional documentation on the behavior of deactivation kinetics as channels inactivate is given in Table II, where the fast time constants of tails after 15- and 300-ms pulses are compared in a number of cells and are found to be essentially identical.

Inactivation Elicited by a More Positive Holding Potential

Partial inactivation of the Ca current can also be caused by holding the membrane potential at −40 mV for seconds or minutes. The remaining current is then assayed by depolarizations from this level. We hesitated to subject cells to this procedure, because it is poorly reversible and caused permanent degradation of the amplitude of the Ca current. For pulses from −40 mV, the Ca current lacked the prominent inactivating component seen with steps from −80 mV. Instead, the current quickly reached a steady amplitude that decayed only slightly in 300 ms. The amplitude was smaller than the amplitude at the end of a 300-ms pulse from −80 mV to the same test potential.

TABLE II

Closing Time Constants

	Test pulse duration*		Test pulse amplitude‡		Repolarization potential	
	15 ms	300 ms	0 mV	+40 mV	−80 mV	−40 mV
τ_f	231 ± 21	230 ± 33	230 ± 29	232 ± 14	172 ± 14	580 ± 32
	n = 11	n = 7	n = 6	n = 6	n = 8	n = 5

τ_f is the time constant of the fast decaying tail component in microseconds. Mean ± SD. n is the number of cells. 5 Ba^{2+}, 10 Mg^{2+}//50 Cs^+, 50 NMG^+, 10 EGTA or 10 BAPTA. 20°C. Repolarization potential was −60 mV.

*Test pulses were from −80 to +20 mV.

‡Test pulse duration, 15 ms.

The lack of a transient component can be interpreted in two ways. It could be that N channels are inactivated and do not contribute to the current for a holding potential of −40 mV, leaving only the HVA channels to carry current. It could equally well be that both transient and steady state currents arise from a single set of channels that inactivate only partially. At a holding potential of −40 mV, the inactivation process is in steady state and proceeds no further during a test pulse.

The ambiguity in interpreting results from this procedure, combined with the fact that, at least in our hands, it damages the cells, makes it not very useful for separating channel types.

Effect of Time in Culture on Ca Current Inactivation

FD channel currents appeared to inactivate faster in older cultures whose cells had processes. Fig. 8 *A* illustrates inactivation in a DRG neuron that was kept for 2 d in culture and had already developed large processes. In these experiments, Na currents were not suppressed, and the first inward peak is Na current. The current decayed from its second (I_{Ca}) peak to ~20% of its size during a 100-ms test pulse

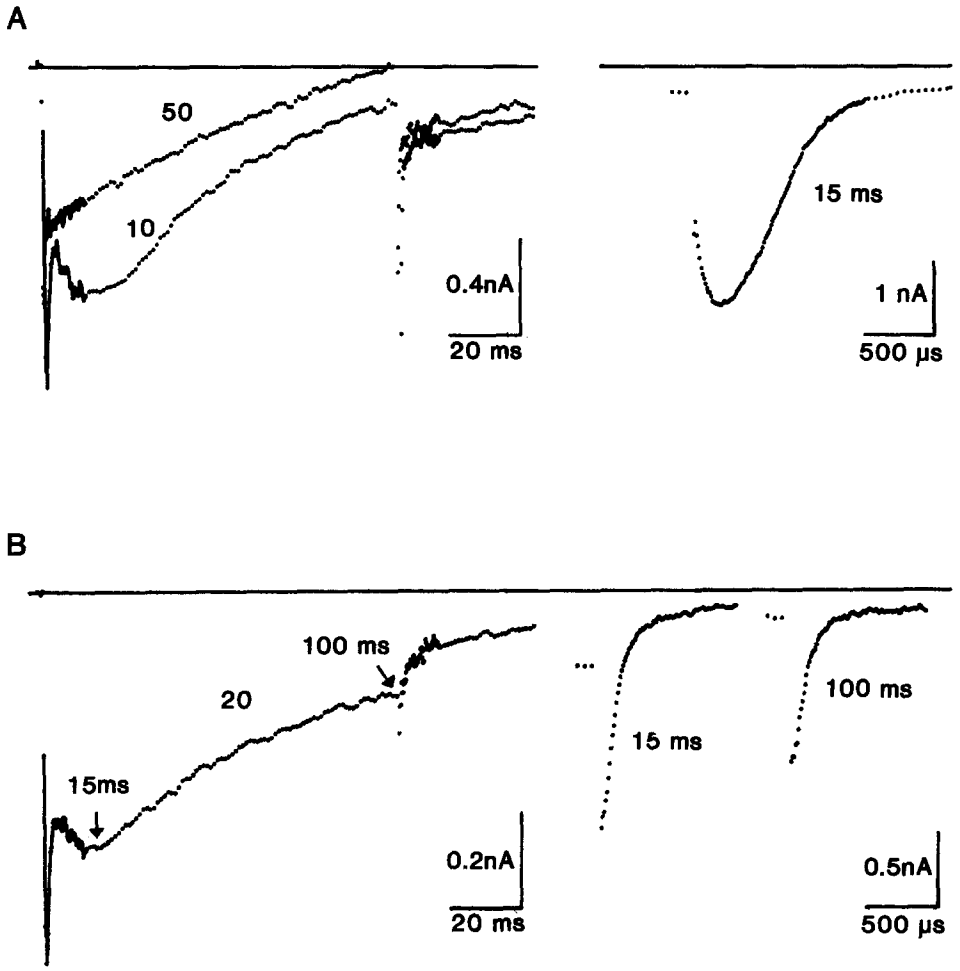

FIGURE 8. Whole-cell currents in DRG neurons with processes. (*Left*) Whole-cell currents were recorded in neurons kept 2 d in culture. Note that Na currents were not blocked in these experiments. 100-ms test pulses were from −80 mV to the potentials indicated. (*Right*) Tail currents were measured on repolarization to −60 mV after test pulses from −80 to +20 mV. Test pulse durations are indicated. 120 NaCl, 20 $CaCl_2$, 2 $MgCl_2$, 10 HEPES//90 Cs glutamate, 20 CsCl, 30 NMG-Cl, 2 $MgCl_2$, 10 EGTA, 10 HEPES. pH was adjusted to 7.3 with Cs(OH). 20°C.

to +10 mV. At +50 mV, the current declined to zero and would have been outward with longer test pulses. Tail current measurements revealed an unusual behavior of channel deactivation in these older preparations. Fig. 8 *A* (right) shows a typical tail current record for this neuron with high time resolution. It was taken on repolarization to −60 mV after a 15-ms test pulse to +20 mV. In contrast to the instantaneous current jump and fast initial relaxation seen in cells without processes, the current in this cell rose slowly to its peak after repolarization and declined over several hundred microseconds.

These observations point to two major problems in recordings from cells with processes. The first is that the ionic content of the processes does not exchange rapidly with the pipette. Thus, in our case, a spurious "inactivation" can result from K current in the processes, where a significant K ion concentration may be retained and may even give rise to outward current. The second problem is that the membrane voltage of the processes is not under control, and this non–space-clamped region gives rise to uninterpretable current patterns, as shown in the tail recording of Fig. 8 *A*.

Similar, but less pronounced, distortions of the tails were seen consistently in all cells with processes, even if the processes were barely visible under the microscope, as in the neuron of Fig. 8 *B*. Current inactivation was also fast in this cell. Tail currents recorded after test pulses of different durations decayed in two phases with no obvious delay. The slow tail component was unusually large and variable, which indicates an inadequate space clamp. Moreover, the decrease in the tail current amplitude with increasing test pulse durations was not proportional to the decrease in the pulse current amplitude, as it invariably was in freshly dissociated cells. As illustrated in Fig. 8 *B*, the pulse current amplitude at 15 ms was reduced by ~60% at the end of the pulse, while the corresponding tail current amplitude was only ~30% smaller at this time. Since, in our hands, all healthy cells at this stage of cultivation possess membrane extensions that make whole-cell recordings uninterpretable, our experiments were restricted to early stages.

Instantaneous I-V Relations for FD Channels

The *I-V* relation for open FD channels was determined with Ba ions as charge carriers. The channels were activated by pulses from −80 to +20 mV for 8 ms. At the end of the activating pulse, a test pulse to different voltages was applied (Fig. 9 *A*); the current amplitude was measured as soon as possible and is plotted as a function of membrane potential. The resulting curve (Fig. 9 *B*) was nonlinear and its slope decreased progressively for voltages above −10 mV. Changing the holding potential to more positive potentials or increasing the duration of the activating pulse to 200–300 ms reduced the current amplitude without changing the shape of the instantaneous *I-V* curve. Thus, it appears that these procedures reduced the number of conducting channels, but, from the point of view of the instantaneous *I-V* relation, the inactivated channels and the still active ones were indistinguishable.

FD Tail Current Kinetics at Different Membrane Potentials

So far, our results have provided evidence for the existence of two populations of Ca channels in DRG neurons. As described in this section, several more tests were conducted to attempt to identify a third type of Ca channel.

The first test examined the voltage dependence of FD channel deactivation. The tail current decay became progressively faster with more negative repolarization potentials. At all potentials tested (between −100 and −10 mV), the decay of the fast tail component was very well fitted with a single exponential after subtracting out a slow exponential when necessary. This is demonstrated in Fig. 10 *A* for two repolarization potentials. Tail currents were recorded on repolarization to −40 and −80 mV after 10-ms voltage steps from −80 to +20 mV. The time constant of

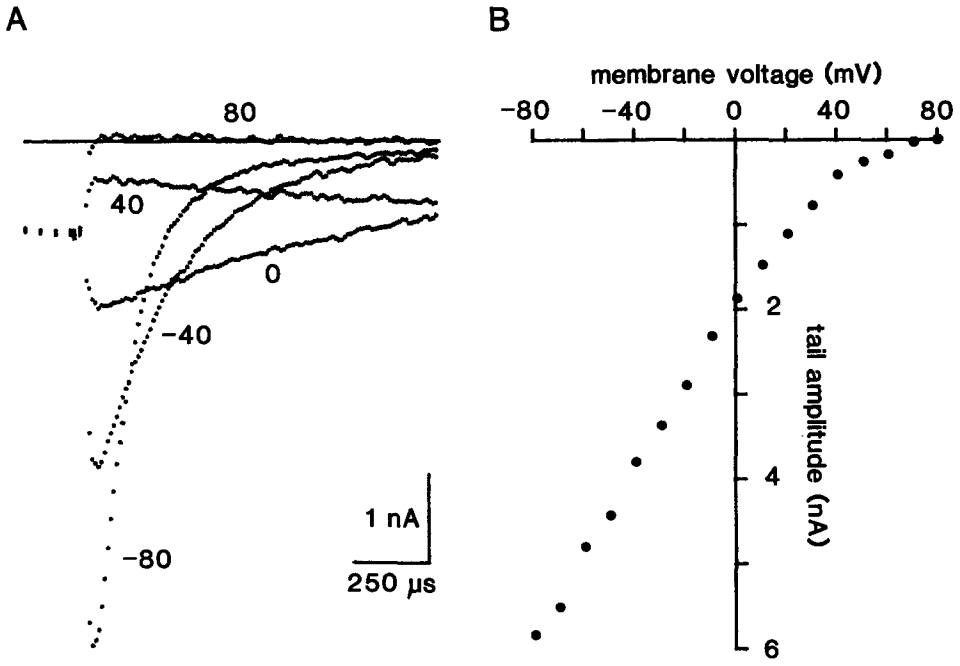

FIGURE 9. Instantaneous *I-V* relation for FD channels. (*A*) Instantaneous currents were measured at a variety of potentials following activation of Ba currents with 10-ms pulses from −80 to +20 mV. (*B*) Tail amplitudes were plotted as a function of the repolarizing potential level. 5 Ba^{2+}, 10 Mg^{2+}//50 Cs^{+}, 50 NMG^{+}, 10 BAPTA. 20°C.

the current decay was substantially larger at −40 mV. For an e-fold change in τ_f, a change in potential of 22 mV was necessary in this neuron. In no case was there evidence for a third tail current component.

FD Tail Current Kinetics Do Not Change with the Degree of Channel Activation

The deactivation kinetics, τ_f, did not change significantly as the channels activated. Fig. 10 *B* shows that the time course of the tail current decay was identical after a 15-ms test pulse that fully activated the channels or after a 4-ms one that activated only 40% of the pulse current. Note the slower current kinetics at 10°C. Variations of the magnitude of the test pulse also failed to produce any changes in the time course of the tail current decay, as illustrated in Fig. 10 *C* with test pulses from −80 to 0 and +40 mV. Table II summarizes the deactivation kinetics of the fast tail

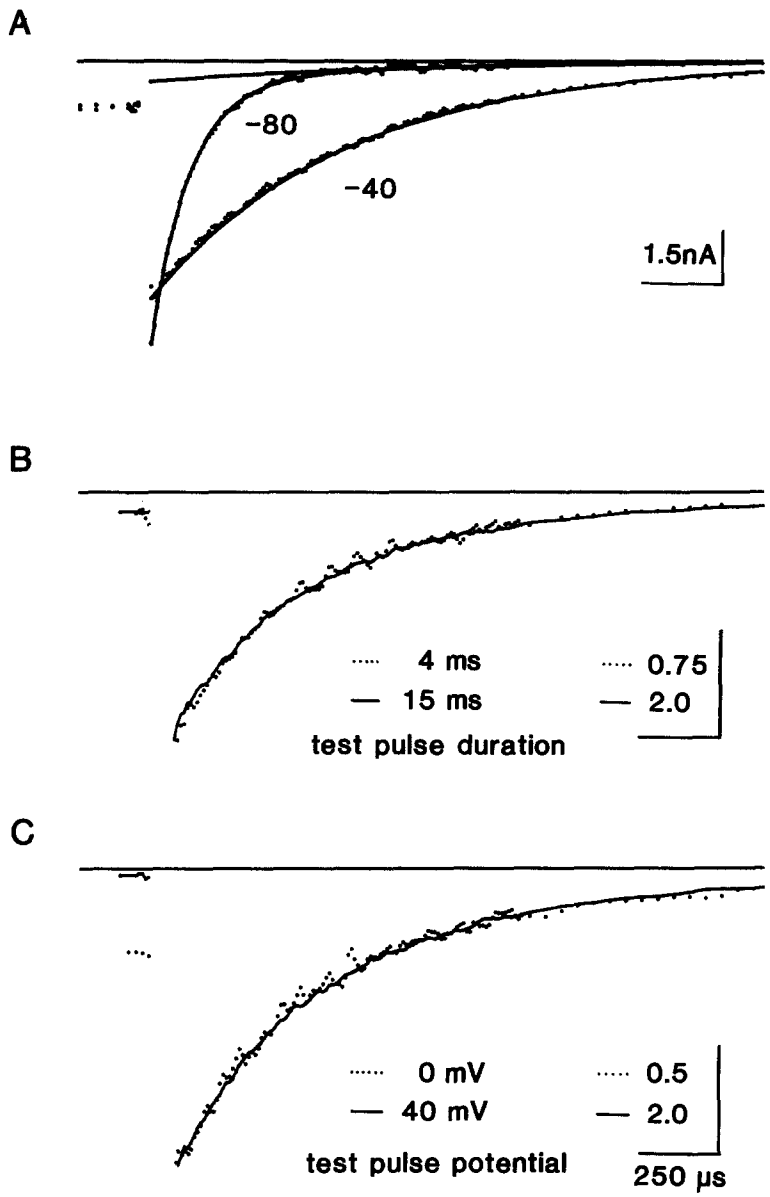

FIGURE 10. Tail currents recorded at different repolarization levels (*A*), after test pulses of variable duration (*B*) and amplitude (*C*). *A* compares tail currents recorded on repolarization to −40 and −80 mV after 10-ms test pulses from −80 to +20 mV. The continuous curves are single and double exponentials fitted to the tail current decay. The fast and slow tail components at −80 mV were fitted with a double exponential. Fitting of the slow component with a single exponential is shown separately. The time constants were 118 µs and 0.74 ms. The tail current decay at −40 mV was fitted best with a single exponential. The time constant was 0.6 ms; 20°C. *B* and *C* show tail currents recorded on repolarization to −60 mV after 4- and 15-ms test pulses from −80 to +20 mV (*B*) and after 15-ms test pulses to 0 and +40 mV (*C*). The dotted traces were scaled and superimposed. The fast tail components were fitted with single exponentials (fits not shown). The time constant was 450 µs in *B* and *C*. (*A*) 5 Ba^{2+}, 10 Mg^{2+}//50 Cs^{+}, 50 NMG^{+}, 10 EGTA. 20°C. (*B* and *C*) 5 Ba^{2+}, 2 Mg^{2+}//50 Cs^{+}, 50 NMG^{+}, 10 BAPTA. 10°C.

component measured at different repolarization potentials and after test pulses of variable duration and amplitude.

Inactivation and Temperature Dependence

The deactivation kinetics, τ_f, of FD channel currents were sensitive to temperature. Fig. 11 illustrates the slowing of the tail current decay at lower temperatures. The

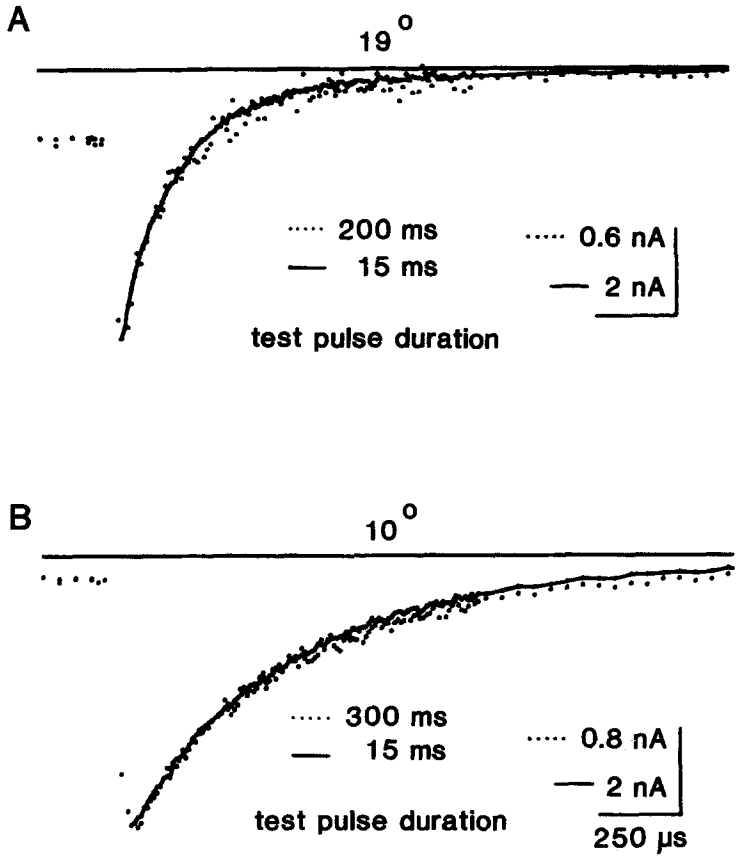

FIGURE 11. Temperature effect on tail currents. Tail currents were measured after test pulses from −80 to 0 (*A*) and +20 mV (*B*) with repolarization to −60 mV. The duration of the activating pulse and the temperature are indicated. Dotted tails, recorded after long pulses that inactivated many channels, were scaled and superimposed. The fast tail components were fitted with single exponentials (fits not shown). The time constant was 235 µs in *A* and 570 µs in *B*. 5 Ba^{2+}, 10 Mg^{2+}//50 Cs^+, 50 NMG^+, 10 BAPTA.

tails were measured after test pulses of 15 and 200 ms at 19°C and of 15 and 300 ms at 10°C. Tail currents in this particular cell had only a fast component, which was easily fitted with a single exponential at both temperatures. The time constant of the current decay decreased by a factor of ~2.5 when the bath temperature was changed by 10°C. It is evident from these results that FD channels behave as a single class of Ca channels over a wide temperature range.

Furthermore, Fig. 11 (cf. Fig. 7) shows that the deactivation kinetics did not change at either temperature as the channels inactivated. The tail currents decayed with the same time constant after a 15-ms activating pulse or after a 200-ms (*A*) or a 300-ms (*B*) pulse, during which the pulse current inactivated to 50 and 40%, respectively. After scaling in amplitude, the currents after 200 or 300 ms superimpose on the 15-ms tail.

DISCUSSION

More Than Two Ca Channels in Chick DRG Neurons?

Recent findings have provided clear evidence for two types of Ca channels in avian sensory neurons (Carbone and Lux, 1984 *a*, *b*). The two types, called LVA and HVA channels, are readily distinguishable on the basis of the voltage range in which they activate, their single-channel conductance, and other properties. In addition, a third type, the N channel, has been described (Nowycky et al., 1985*a*) that has properties intermediate between the two established types. Like the LVA channels, N channels inactivate relatively rapidly, but they activate in about the same voltage range as HVA channels. Thus, N channels are seen when the holding potential is relatively negative and the test potential is relatively positive.

Because their properties overlap with the other two channel types, it is difficult to isolate N channel currents in macroscopic current recordings. According to the published curves (Fox et al., 1987), it seems impossible to inactivate N channels completely by changing the holding potential without partially inactivating HVA channels. Nor does the kinetic evidence on inactivation allow a clear demonstration for the existence of N channels. Inactivation shows a fast (~80 ms) and a slow (hundreds of milliseconds) time constant (see Nowycky et al., 1985*a*). Without supporting evidence, one cannot be sure whether a fast and a slow component of inactivation result from the presence of two channel types (HVA and N) or from two inactivation processes affecting a single type of channels. There is, for instance, a fast and slow inactivation of Na and Ca channels.

Further, neither inorganic nor organic Ca channel blockers have proved helpful in isolating N channels. While, for example, micromolar concentrations of Ni^{2+} block LVA channels selectively (Carbone et al., 1987), no selective agent for the N channels has so far been found. Nifedipine, a dihydropyridine, is said to preferentially inhibit L channels, but block occurs only after prolonged depolarization to potentials where most of the N channels are inactivated (Rane et al., 1987). Therefore, one cannot be sure whether N channels in these circumstances are blocked or not blocked, because they are inactivated. Nifedipine effects thus do not provide evidence for the existence of N and HVA channels. Another dihydropyridine, Bay K 8644, said to selectively affect HVA channels, has so far proved ineffective in our hands when applied to chick DRG neurons.

Against this background of uncertainty regarding macroscopic N currents, single-channel measurements assume great importance. Several types of unitary events have been resolved from cell-attached patches formed with high Ba^{2+} concentrations in the pipette (Nowycky et al., 1985*a*; Carbone and Lux, 1987*b*). There is more than one interpretation of these measurements in the literature. While Nowycky et

al. identified unit events with a conductance of 13 pS in 110 Ba^{2+} as N channels, Carbone and Lux raise the question of whether these events represent a second conductance state of a unique channel type, the HVA channel. In a similar vein, Nowycky et al. (1985*b*) argue that there are two modes of gating of HVA channels and that Bay K 8644 shifts the distribution between modes. Further, it remains to be demonstrated convincingly that the unitary events said to be of the N type correspond to the macroscopic N current, which is recorded under quite different ionic conditions.

In an attempt to clarify these questions regarding N channels, we have chosen to study a different aspect of channel behavior, the closing or deactivation kinetics, inferred from the tail currents.

Two Ca Tail Current Components in DRG Neurons

Like Ca tail currents in pituitary cells (Matteson and Armstrong, 1984*a*, 1986; Armstrong and Matteson, 1985; Cota, 1986), Ca tail currents in chick DRG neurons decay in two clearly distinct phases (see also Carbone and Lux, 1987*a*). Under no circumstances was there evidence for a third tail component of significant size (Fig. 7 and Table II). The main evidence we sought was a change in tail kinetics upon inactivation of the N channels, as discussed below. Weaker evidence for an additional channel type would be the existence of two exponential components in the fast part of the tail—weaker because a single channel type can in theory generate a multiexponential tail. Nonetheless, after removing the slow component, which is easily separated because of its slow time constant, the remaining current was always well fitted by a single exponential, leaving only an extremely small residual current. In an attempt to fit two exponentials to the fast tail, the fitting routine assigned an amplitude of zero to the second exponential.

The decay kinetics of the fast tail component are not changed by inactivation or by varying the degree of activation. Taken together, these observations lead to the conclusion that either the fast tail component is due to deactivation of one population of Ca channels, i.e., HVA channels, or that the closing kinetics of HVA and N channels are identical. However, as shown here, this identical behavior is not limited to certain potentials, but instead extends over a wide range of membrane potentials (see Figs. 9 and 10). Moreover, neither variations in the amplitude or duration of activating and inactivating pulses (Figs. 7, 10, and 11) nor changes in temperature (Fig. 11) revealed more than one rapidly deactivating tail component. These findings strongly suggest that FD channels in chick DRG neurons represent one population of Ca channels with properties similar to HVA channels. The possibility of two channels with identical deactivation kinetics under all the conditions employed seems remote but cannot be ruled out. Are all of the observed channels of the N type? This seems unlikely, because N channels inactivate completely (Nowycky et al., 1985*a*).

Do N Channels Develop with Time in Culture?

N channel currents were described in DRG neurons maintained for several days in culture (Nowycky et al., 1985*a*). One possible explanation for the lack of N channels in our preparation could be the short period (6–12 h) during which these neurons

were kept in culture after dissociation, or the lack of processes, which might be enriched with N channels. We have therefore attempted to examine Ca currents in older cells. However, as demonstrated in Fig. 8, macroscopic current recordings, particularly current kinetics, are uninterpretable at this stage of cultivation. Tail kinetics are badly distorted by current contributed from the processes that are not under voltage control, because of their distance from the soma. Further, it appears that the processes may still contain an appreciable concentration of K ions and thus yield an outward current that contributes to the appearance of inactivation. Thus, voltage-clamp records from cells with processes are extremely difficult, if not impossible, to interpret. The remote regions have an unknown ionic environment, unknown and inconstant voltage, and an unkown complement of channels in the membrane.

Since there is no macroscopic evidence for a third type of Ca channel in freshly dissociated neurons and we consider records from older ones to be uninterpretable, single-channel data remain the only basis on which to establish the existence of N channels. In particular, the reconstruction of macroscopic N-type currents from single-channel currents would be required. Macroscopic reconstructions have been done (Nowycky et al., 1985*a*), but the inactivation kinetics of the reconstructed currents are similar to those of LVA or T channels, i.e., much faster than for the macroscopic N current in the same neurons.

We thank Dr. Martin Pring for statistical advice and for performing the Fletcher-Powell fitting to our data. We further thank Dr. R. W. Tsien for providing us with a preprint of the article by Fox et al. (1987).

This work was supported by National Institutes of Health grant NS-12543 to C. M. Armstrong and a grant of the Max Kade Foundation to D. Swandulla.

Original version received 31 August 1987 and accepted version received 11 March 1988.

REFERENCES

Adams, D. J., and P. W. Gage. 1977. Calcium channel in *Aplysia* nerve cell membrane: ionic and gating current kinetics. *Proceedings of the Australian Physiological and Pharmacological Society.* 8–28P.

Armstrong, C. M., and R. H. Chow. 1987. Supercharging: a method for improving patch-clamp performance. *Biophysical Journal.* 51:133–136.

Armstrong, C. M., and D. R. Matteson. 1985. Two distinct populations of calcium channels in a clonal line of pituitary cell. *Science.* 227:65–67.

Bean, B. P. 1985. Two kinds of calcium channels in canine atrial cells. *Journal of General Physiology.* 86:1–31.

Bossu, J. L., A. Feltz, and J. M. Thomann. 1985. Depolarization elicits two distinct calcium currents in vertebrate sensory neurons. *Pflügers Archiv.* 403:360–368.

Carbone, E., and H. D. Lux. 1984*a*. A low voltage-activated calcium conductance in embryonic chick sensory neurons. *Biophysical Journal.* 46:413–418.

Carbone, E., and H. D. Lux. 1984*b*. A low voltage-activated, fully inactivating Ca channel in vertebrate sensory neurones. *Nature.* 310:501–502.

Carbone, E., and H. D. Lux. 1987*a*. Kinetics and selectivity of a low-voltage-activated calcium current in chick and rat sensory neurones. *Journal of Physiology.* 386:547–570.

Carbone, E., and H. D. Lux. 1987*b*. Single low-voltage-activated calcium channels in chick and rat sensory neurones. *Journal of Physiology.* 386:571–601.

Carbone, E., M. Morad, and H. D. Lux. 1987. External Ni^{2+} selectively blocks the low-threshold Ca^{2+} currents of chick sensory neurons. *Pflügers Archiv.* 408:R60.

Cota, G. 1986. Calcium channel currents in pars intermedia cells of the rat pituitary gland. *Journal of General Physiology.* 88:83–105.

Deitmer, J. W. 1984. Evidence for two voltage-dependent calcium currents in the membrane of the ciliate *Stylonychia. Journal of Physiology.* 355:137–159.

DeRiemer, S. A., and B. Sakmann. 1986. Two calcium currents in normal rat anterior pituitary cells identified by a plaque assay. *In* Calcium Electrogenesis and Neuronal Functioning. U. Heinemann, M. Klee, E. Neher, and W. Singer, editors. Springer-Verlag, Heidelberg. 139–154.

Fedulova, S. A., P. G. Kostyuk, and N. S. Vesclovsky. 1985. Two types of calcium channels in the somatic membrane of new-born rat dorsal root ganglion neurones. *Journal of Physiology.* 359:431–446.

Fenwick, E. M., A. Marty, and E. Neher. 1982. Sodium and calcium channels in bovine chromaffin cells. *Journal of Physiology.* 331:599–635.

Fishman, M. C., and I. Spector. 1981. Potassium current suppression by quinidine reveals additional calcium currents in neuroblastoma cells. *Proceedings of the National Academy of Sciences.* 78:5245–5249.

Fox, A. P., and S. Krasne. 1981. Two calcium currents in egg cells. *Biophysical Journal.* 33:145*a*. (Abstr.)

Fox, A. P., and S. Krasne. 1984. Two calcium currents in *Neanthes arenacoedentatus* egg cell membranes. *Journal of Physiology.* 356:491–505.

Fox, A. P., M. C. Nowycky, and R. W. Tsien. 1987. Kinetic and pharmacological properties distinguishing three types of calcium currents in chick sensory neurones. *Journal of Physiology.* 394: 149–172.

Hagiwara, S., and L. Byerly. 1981. Calcium channels. *Annual Review of Neuroscience.* 4:69–125.

Hagiwara, S., S. Ozawa, and O. Sand. 1975. Voltage-clamp analysis of two inward current mechanisms in the egg cell membrane of a starfish. *Journal of General Physiology.* 65:617–644.

Hamill, O., A. Marty, E. Neher, B. Sakmann, and F. J. Sigworth. 1981. Improved patch-clamp techniques for high-resolution current recording from cells and cell-free membrane patches. *Pflügers Archiv.* 391:85–100.

Kostyuk, P. G., O. A. Krishtal, and V. I. Pidoplichko. 1977. Asymmetrical displacement currents in nerve cell membrane and effect of internal fluoride. *Nature.* 367:70–72.

Llinas, R., and M. Sugimori. 1980. Electrophysiological properties of in vitro Purkinje cell somata in mammalian cerebellar slices. *Journal of Physiology.* 305:171–195.

Llinas, R., and Y. Yarom. 1981. Electrophysiology of mammalian inferior olivary neurones in vitro. Different types of voltage dependent ionic conductances. *Journal of Physiology.* 315:549–567.

Matteson, D. R., and C. M. Armstrong. 1984*a*. Evidence for two types of Ca channels in GH3 cells. *Biophysical Journal.* 45:36*a*. (Abstr.)

Matteson, D. R., and C. M. Armstrong. 1984*b*. Na and Ca channels in a transformed line of anterior pituitary cells. *Journal of General Physiology.* 83:371–394.

Matteson, D. R., and C. M. Armstrong. 1986. Properties of two types of calcium channels in clonal pituitary cells. *Journal of General Physiology.* 87:161–182.

Mitra, R., and M. Morad. 1986. Two calcium channels in guinea pig ventricular myocytes. *Proceedings of the National Academy of Sciences.* 3:5340–5344.

Narahashi, T., A. Tsunoo, and M. Yoshii. 1987. Characterization of two types of calcium channels in mouse neuroblastoma cells. *Journal of Physiology.* 383:231–249.

Nilius, B., P. Hess, J. B. Lansman, and R. W. Tsien. 1985. A novel type of cardiac calcium channel in ventricular cells. *Nature.* 316:443–446.

Nowycky, M. C., A. P. Fox, and R. W. Tsien. 1985*a*. Three types of neuronal calcium channel with different calcium agonist sensitivity. *Nature.* 316:440–443.

Nowycky, M. C., A. P. Fox, and R. W. Tsien. 1985*b*. Long-opening mode of gating of neuronal calcium channels and its promotion by the dihydropyridine calcium agonist Bay K 8644. *Proceedings of the National Academy of Sciences.* 82:2178–2182.

Rane, S. G., G. G. Holz IV, and K. Dunlap. 1987. Dihydropyridine inhibition of neuronal calcium current and substance P release. *Pflügers Archiv.* 409:361–366.

Swandulla, D., and C. M. Armstrong. 1987. Calcium channel tail currents in chick sensory neurons. *Neuroscience Abstracts.* 13:4099.